Chemical Engineering and Processing 102 (2016) 102–116

Contents lists available at ScienceDirect

Chemical Engineering and Processing: Process Intensification

journal homepage: www.elsevier.com/locate/cep

# Hydrodynamics and mixing in continuous oscillatory flow reactors—Part II: Characterisation methods

A. Mazubert[a,b], D.F. Fletcher[c], M. Poux[a,b], J. Aubin[a,b,*]

[a] University of Toulouse, INPT/UPS, Laboratoire de Génie Chimique, 4 Allée Emile Monso, BP-31243, 31432 Toulouse, France
[b] CNRS, Laboratoire de Génie Chimique, 31432 Toulouse, France
[c] School of Chemical and Biomolecular Engineering, The University of Sydney, NSW 2006, Australia

ARTICLE INFO

*Article history:*
Received 28 August 2015
Received in revised form 17 December 2015
Accepted 18 January 2016
Available online 21 January 2016

*Keywords:*
Mixing
Process intensification
Oscillatory baffled reactors
Oscillatory flow

ABSTRACT

This work presents and exploits quantitative measures to better quantify the performance of oscillatory baffled reactors, being complementary to simple vector plots and shear strain rate fields. Novel performance criteria, including radial and axial fluid stretching and mixing, as well as the shear strain rate history of fluid elements have been developed and used to compare the performance of five different baffle designs, namely single orifice baffles, disc-and-donut baffles and three novel variations of helical blades. Analysis of residence time distributions has also been used to evaluate the geometries. The performance measures highlight that the disc-and-donut baffles can provide significant shear strain rates, which could be useful for multiphase applications, but also significant axial dispersion that is comparable with that for the single orifice baffles. The results also suggest that helical blade designs could be promising for decreasing axial dispersion, whilst maintaining significant levels of shear strain rate.



## 1. Introduction

In Part I of this series [1], time-resolved laminar CFD simulations have been performed to study the flow generated in five oscillatory baffled reactor (OBR) designs, three of which are novel compared with the single orifice baffles or disc-and-donut baffles that have been traditionally used for this type of device. The flow generated by these designs has been assessed by examining instantaneous velocity fields, shear strain rate fields and pressure drop.

This study highlighted the complex flow behavior and the formation of vortices in the reactor due to both flow blockage by the baffle design and flow reversal. Indeed, depending on the baffle geometry, there is more or less fluid recirculation, dominant axial flow and shear strain rate variation. The disc-and-donut baffles generate multiple vortices and the helical blade designs create a complex 3D flow with a significant transverse component. In terms of shear strain rates, which are of interest for multiphase applications, the disc-and-donut baffles and the helical blade baffles provide the highest values, which are more than two times greater than those generated by the single orifice design. It is interesting to note however that the maximum strain rates are localised and occupy relatively small volumes in the reactor; only the disc-and-donut baffles provide substantial spatial variation of shear strain rate. This means that only a small amount of fluid passing through the reactor may experience high shear stress. The work also showed that the baffle design has a huge impact on pressure drop, which is as expected. The disc-and-donut design causes the highest pressure drop, which is greater by about a factor of five than that with the single orifice baffles. The pressure drop generated by helical baffles is approximately half that of the disc-and-donut design. Indeed, although the ensemble of the results provide knowledge on the flow mechanisms and operating characteristics of OBRs, it is clearly difficult to conclude on the impact of baffle design on the performance of the reactor with velocity and shear strain rates alone.

As previously reported in the introduction of Part I, the majority of the studies in the literature describe the flow generated in OBRs in a qualitative manner using planar velocity fields and velocity profiles [2–5] or shear strain rate fields [6]. A significant number of studies have also evaluated the performance of OBRs in terms of axial dispersion via the analysis of residence time distributions [7–13]. The general observation of these studies is that for oscillatory Reynolds numbers ($Re_O$) greater than approximately 200, the axial dispersion coefficient increases linearly when with increasing $Re_O$, being proportional

* Corresponding author at: CNRS, Laboratoire de Génie Chimique, 31432 Toulouse, France.
*E-mail address:* joelle.aubincano@ensiacet.fr (J. Aubin).

http://dx.doi.org/10.1016/j.cep.2016.01.009
0255-2701/© 2016 Elsevier B.V. All rights reserved.

**Nomenclature**

| | |
|---|---|
| $A$ | Amplitude of oscillation (m) |
| $d$ | Tube diameter (m) |
| $D_{ax}$ | Axial dispersion coefficient ($m^2\,s^{-1}$) |
| $E$ | Residence time distribution ($s^{-1}$) |
| $f$ | Frequency of oscillation (Hz) |
| $\boldsymbol{F}_D$ | Drag force (N) |
| $l$ | Stretching distance (m) |
| $L$ | Length of tube (m) |
| $m_p$ | Mass of particle (kg) |
| $n_{pairs}$ | Number of particle pairs |
| $N_w$ | Weighted number of particles |
| Pe | Péclet number ($u\,L/D_{ax}$) |
| $Q$ | Volumetric flow rate ($m^3\,s^{-1}$) |
| $R$ | Radial location (m) |
| $Re_{net}$ | Net Reynolds number ($u_{net}d\rho/\mu$) |
| $Re_O$ | Oscillatory Reynolds number ($2\pi fAd\rho/\mu$) |
| $S_{ij}$ | Shear strain rate tensor ($s^{-1}$) |
| SSR | Magnitude of shear strain rate ($s^{-1}$) |
| STD | Standard deviation |
| $t$ | Time (s) |
| $t_m$ | Mean residence time (s) |
| $u$ | Characteristic speed of flow ($m\,s^{-1}$) |
| $\boldsymbol{v}$ | Velocity vector ($m\,s^{-1}$) |
| $V$ | Reactor volume ($m^3$) |
| $X$, $Y$, $Z$ | Cartesian coordinates (m) |
| $\boldsymbol{y}$ | Particle location (m) |

Greek symbols

| | |
|---|---|
| $\mu$ | Dynamic viscosity (Pa s) |
| $\rho$ | Fluid density ($kg\,m^{-3}$) |
| $\sigma_l$ | Standard deviation of stretching distance (m) |
| $\tau$ | Space time ($V/Q$) (s) |

Subscripts

| | |
|---|---|
| 0 | Constant component |
| net | Net |
| o | Oscillatory |

to the product $A.f$. For $Re_O < 200$, however, a decrease in $Re_O$ also causes an increase in the axial dispersion coefficient such that there is a minimum axial dispersion as a function of $Re_O$. Smith and Mackley [9] explain the minimum in the axial dispersion coefficient due to the interaction of net flow and oscillatory flow whereby significant radial mixing is generated without excessive axial mixing. They have also shown that an increase of the net Reynolds number ($Re_{net}$) also causes an increase in the axial dispersion coefficient.

The main objective of this paper is to develop alternative methods that allow OBRs to be characterised and assessed in terms of different performance criteria: radial and axial fluid stretching and mixing, and shear strain rate history. The performance of these methods is then demonstrated using the five different reactor geometries presented in Part 1. A Lagrangian particle tracking method has also been used to carry out an analysis of the residence time distribution, which completes various studies in the literature [9–12,14,15].

## 2. Flow computation and particle tracking

The methodology used to perform the flow simulations was described fully in Part 1 of this paper [1]. In addition to the usual analysis of the flow field variables we also performed Lagrangian particle tracking to provide additional information. We used particles having the same density as the fluid and a diameter of 1 micron which have a Stokes numbers of $O(10^{-5})$ and therefore follow the fluid faithfully. With this method there is no interaction between particles and no physical and little numerical diffusion. The Lagrangian approach introduces no artificial diffusion and in Part I we showed the flow results are mesh and time-step independent so we can reasonably expect the numerical diffusion in the velocity field to be very low. The particle behavior is determined by integration of the kinematic and momentum balance equations for each particle, which take the form

$$\frac{d\mathbf{y}}{dt} = \mathbf{v}, m_p\frac{d\mathbf{v}}{dt} = \mathbf{F}_D \quad (1)$$

where $\mathbf{y}$ is the particle location, $\mathbf{v}$ its velocity, $t$ is time, $m_p$ is the mass of the particle $\boldsymbol{F}_D$ is the drag force, which was modeled using the Schiller Naumann model. These equations were integrated using a fourth-order Runge–Kutta scheme with adaptive step size.

A line of such particles was released along the tube radius at a particular axial location ($X_0$), with their initial velocity set to that of the local fluid velocity. The number of initial particle locations along the line was set at 2484 for 2D geometries and 4968 for 3D geometries and this number of particles proved sufficient to characterise the flow. In addition to recording the particle travel time, location and velocity components, a particle scalar was used to store the local strain rate of the fluid. At the end of the run data

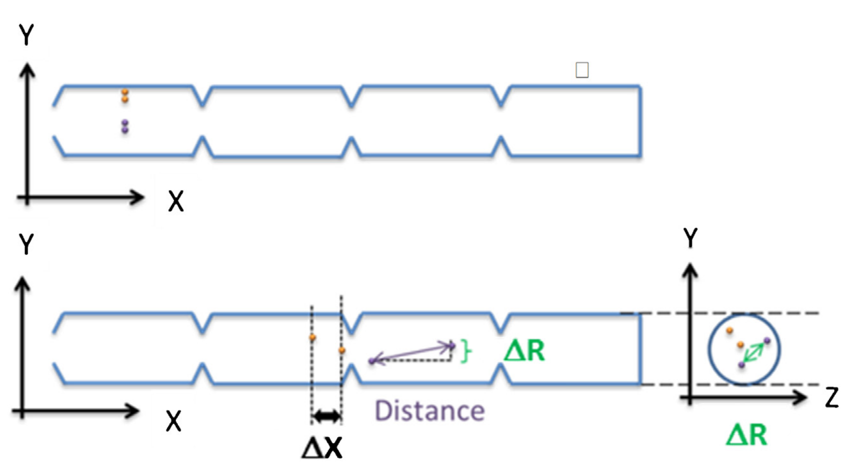


**Fig. 1.** Principle of the radial and axial stretching calculations. At a given time, the axial distance $\Delta X$, and the radial distance $\Delta R$ separating each pair of particles are calculated.